Electronic Supporting Information

Asymmetric Phase Transitions in Lipid Bilayers: Coupling or Budding?

Mona Krompers[1], Miriam Jaki[1], Sinja Götz[1], Jan Lembeck[1], Laurine Kaul[1], Martin Holzer[1] and Heiko Heerklotz[1,2,3]

[1] University of Freiburg, Institute of Pharmaceutical Sciences, Freiburg, Germany
[2] University of Toronto, Leslie Dan Faculty of Pharmacy, Toronto, Canada
[3] Signaling Research Center BIOSS, Freiburg, Germany

Contents

1. HPLC analysis of SOPC/DPPG vesicles – protocol validation

We developed a HPLC method as a fast and reliable tool for specific SOPC and DPPG quantification. The validation results confirm a wide working range, high accuracy, and acceptable precision.

Specificity. A forced degradation study was conducted to ensure sufficient separation of the analytes from their degradation products. For this purpose, SOPC and DPPG were incubated for 5 hours in 0.5% NaOH prior to HPLC analysis (Figure S1). There were no interferences of the analytes with the detected degradation products.

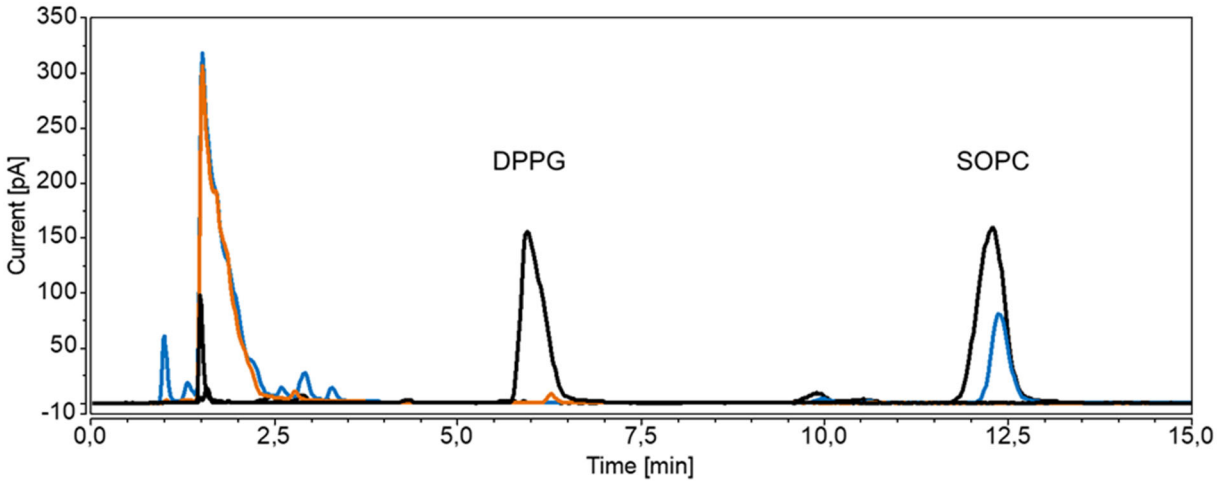

Figure S1: HPLC validation: forced degradation. Chromatograms of pure SOPC and pure DPPG (both black) overlaid with samples incubated in 0.5% NaOH (blue: SOPC; orange: DPPG). No degradation peak interfered with sample peaks.

Working Range – Calibration. A seven-point calibration for the quantification of SOPC and DPPG was conducted using lipid stock solutions of 10 to 1000 µg/mL in ethanol. The resulting peak area was plotted against the concentration to obtain the calibration curves presented in Figure S2. Raw data is displayed in Figure S2. It is well known that charged aerosol detectors (CAD) show non-linear response when applied over a large concentration range [1,2]. Therefore, the use of a quadratic fit is an adequate and ICH accepted approach for CAD response calibration [3–6]. Calibration was successful, as indicated by high R^2 values (> 0.9998) for the quadratic fits.

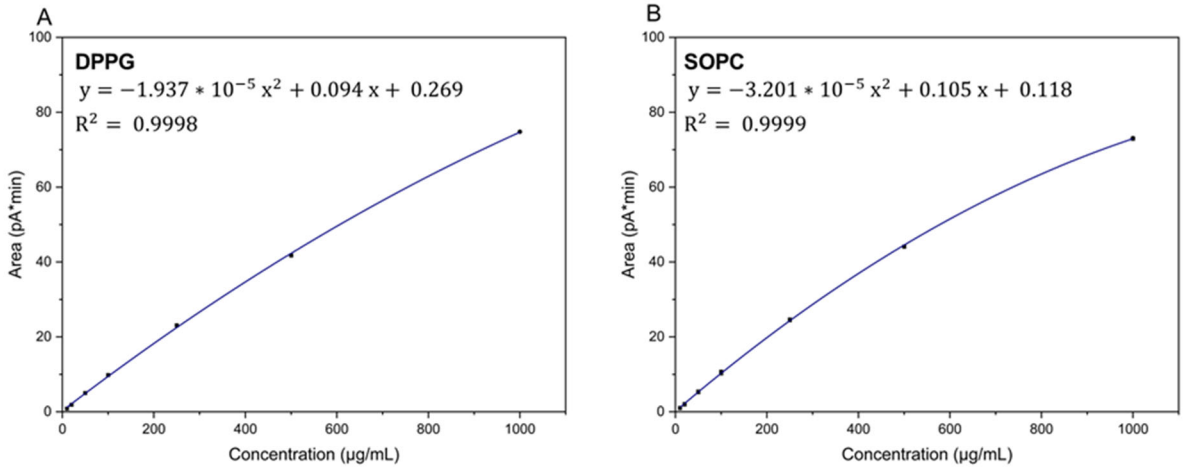

Figure S2: HPLC validation: calibration curves for DPPG (A) and for SOPC (B). A quadratic fit was applied as shown in the graphs.

Working Range – Lower Range Limits. Detection Limit (DL) and quantitation limit (QL) were determined based on the signal-to-noise ratio of calibration samples with known, low concentrations (10 µg/mL). A signal-to-noise ratio of 10 is required for quantitation, whereas a signal-to-noise ratio of 3 is sufficient for detection [6].

The HPLC method has low detection and quantitation limits as displayed in Table S 1. This ensures a wide working range suitable for many types of asymmetric liposomes.

Table S 1: HPLC validation: lower range Limits. Detection limit (DL) and quantitation limit (QL) of DPPG and SOPC were calculated based on the signal-to-noise ratio of calibration samples with low concentrations. Data is shown as mean ± SD (DPPG n=9; SOPC n=6).

Component	DL (µg/mL)	QL (µg/mL)
DPPG	0.29 ± 0.04	0.98 ± 0.13
SOPC	0.68 ± 0.11	2.27 ± 0.36

Precision. Determining precision is important to quantify variations originating from the HPLC method. Two types of precision were examined: repeatability, known as intra-day variability between injections of the same sample on the same day, and intermediate precision, which investigates inter-day variability such as eluent preparation and varying room temperature.

Repeatability was determined analyzing samples of SOPC and DPPG at three different concentration levels (SOPC: 100, 200, 400 µg/mL; DPPG: 125, 250, 500 µg/mL) three times on the same day. For intermediate precision, these samples were injected again, three times each, on two other days. Repeatability was calculated as the mean intra-day variability of all three days. Intermediate precision was calculated from the means of the three separate days. Both repeatability and intermediate precision were calculated regarding retention time and peak area. Raw chromatography data for the calculations are presented in Table S6.

The retention time of both DPPG and SOPC were precise with RSD < 1.63, as shown in Table S 2.

Table S 2: HPLC Validation: Precision of Retention Time. Repeatability and intermediate precision of the retention time of DPPG and SOPC were determined with concentrations of 100, 200, and 400 µg/mL for SOPC and 125, 250, and 500 µg/mL for DPPG. Data is shown in accordance with ICH Q2(R2) requirements as mean ± SD, relative standard deviation (RSD), and mean ± confidence interval (CI) (α=5%); n=3.

Component	Concentration (µg/mL)	Repeatability			Intermediate Precision		
		Mean ± SD (min)	RSD (%)	CI (95%) (min)	Mean ± SD (min)	RSD (%)	CI (95%) (min)
DPPG	125	6.07 ± 0.00	0.03	6.16 ± 0.01	6.06 ± 0.10	1.62	6.06 ± 0.24
	250	5.86 ± 0.02	0.29	6.00 ± 0.02	6.00 ± 0.10	1.63	5.97 ± 0.24
	500	5.80 ± 0.01	0.15	5.93 ± 0.02	5.88 ± 0.08	1.28	5.88 ± 0.19
SOPC	100	12.31 ± 0.01	0.08	12.49 ± 0.02	12.43 ± 0.10	0.79	12.43 ± 0.24
	200	12.34 ± 0.01	0.10	12.48 ± 0.03	12.43 ± 0.08	0.61	12.43 ± 0.19
	400	12.39 ± 0.01	0.12	12.47 ± 0.02	12.44 ± 0.05	0.37	12.44 ± 0.11

The HPLC method showed excellent repeatability of the peak area with a maximum relative standard deviation (RSD) of 0.83% (see Table S3). Intermediate precision was lower but acceptable at low sample concentrations (RSD < 3.43%). This is a phenomenon that has already been observed with CAD and ELSD detectors at low concentration levels [7,8].

Table S 3: HPLC Validation: Precision of Area. Results of repeatability and intermediate precision of SOPC and DPPG at three concentration levels are displayed. Data is shown in accordance with ICH Q2(R2) requirements as mean ± SD, relative standard deviation (RSD), and mean ± confidence interval (CI) (α=5%); n=3.

Component	Concentration (µg/mL)	Repeatability			Intermediate Precision		
		Mean ± SD (pA*min)	RSD (%)	CI (95%) (pA*min)	Mean ± SD (pA*min)	RSD (%)	CI (95%) (pA*min)
DPPG	125	12.09 ± 0.10	0.83	11.91 ± 0.09	12.16 ± 0.30	2.47	12.16 ± 0.75
	250	22.18 ± 0.04	0.20	23.45 ± 0.87	22.61 ± 0.73	3.22	22.61 ± 1.81
	500	41.67 ± 0.07	0.18	41.68 ± 0.05	41.53 ± 0.26	0.62	41.53 ± 0.64
SOPC	100	10.37 ± 0.05	0.43	10.48 ± 0.05	10.22 ± 0.35	3.43	10.22 ± 0.87
	200	20.70 ± 0.06	0.28	20.39 ± 0.22	20.30 ± 0.45	2.22	20.30 ± 1.12
	400	36.98 ± 0.09	0.25	37.33 ± 0.08	37.01 ± 0.31	0.84	37.01 ± 0.77

Accuracy. Accuracy was determined using lipid samples with concentrations of 100, 200, and 400 µg/mL and comparing recovered concentration and anticipated concentration (for raw data, see Table S7). The HPLC method showed sufficient accuracy of 99.32% - 102.67% as shown in Table S 4.

Table S 4: HPLC Validation: Accuracy of DPPG and SOPC Quantification. Shown is the deviation of the analyzed concentration from the expected concentration at 100, 200, and 400 µg/mL. Data is shown in accordance with ICH Q2(R2) requirements as mean ± SD, and mean ± confidence interval (CI) (α=5%); n=3.

Component	Concentration (µg/mL)	Mean % recovery ± SD	Mean % recovery ± CI (95%)
DPPG	100	100.94 ± 3.03	100.94 ± 7.53
	200	101.66 ± 1.25	101.66 ± 3.10
	400	99.86 ± 1.74	99.86 ± 4.32
SOPC	100	99.32 ± 2.67	99.32 ± 6.63
	200	100.96 ± 2.59	100.96 ± 6.43
	400	102.67 ± 3.66	102.67 ± 9.08

2. HPLC Raw Data.

Table S 5: Raw data of HPLC calibration (left: DPPG, right: SOPC; Ret.Time = retention time, S/N = signal-to-noise ratio). Samples of 10-1000 µg/mL SOPC/DPPG were injected.

Injection Name	Ret. Time (min) DPPG	Amount (µg/mL) DPPG	Area (pA*min) DPPG	S/N DPPG	Injection Name	Ret. Time (min) SOPC	Amount (µg/mL) SOPC	Area (pA*min) SOPC	S/N SOPC
1000 DPPG	5.50	1001.81	74.78	507	1000 SOPC	12.34	1003.53	73.08	889
					1000 SOPC	12.34	1002.91	73.06	716
					1000 SOPC	12.34	999.62	72.92	1084
500 DPPG	5.64	492.45	41.75	482	500 SOPC	12.38	494.55	44.13	842
					500 SOPC	12.38	494.08	44.10	838
					500 SOPC	12.38	494.20	44.11	751
250 DPPG	5.74	257.13	23.10	555	250 SOPC	12.47	252.85	24.58	515
					250 SOPC	12.48	253.59	24.64	601
					250 SOPC	12.47	251.55	24.46	511
100 DPPG	5.82	104.04	9.82	258	100 SOPC	12.48	102.69	10.55	229
					100 SOPC	12.48	102.66	10.54	262
					100 SOPC	12.48	102.71	10.55	171
					100 SOPC	12.49	99.93	10.27	235
					100 SOPC	12.49	101.43	10.42	382
					100 SOPC	12.48	100.71	10.35	282
					100 SOPC	12.48	103.46	10.62	239
					100 SOPC	12.48	104.28	10.70	402
					100 SOPC	12.49	104.02	10.68	314
50 DPPG	5.84	50.97	5.00	146	50 SOPC	12.50	50.83	5.36	214
					50 SOPC	12.46	51.11	5.39	175
					50 SOPC	12.46	49.94	5.27	132
					50 SOPC	12.48	50.04	5.28	208
					50 SOPC	12.48	49.56	5.23	126
					50 SOPC	12.48	50.11	5.29	137
					50 SOPC	12.49	51.37	5.42	230
					50 SOPC	12.49	51.01	5.38	204
					50 SOPC	12.48	50.84	5.36	200
20 DPPG	5.87	17.33	1.89	105	20 SOPC	12.50	18.59	2.06	64
					20 SOPC	12.49	18.85	2.08	88
					20 SOPC	12.48	18.99	2.10	90

					20 SOPC	12.50	18.74	2.07	96
					20 SOPC	12.48	18.57	2.05	76
					20 SOPC	12.49	18.35	2.03	82
					20 SOPC	12.49	17.75	1.97	44
					20 SOPC	12.48	18.64	2.06	88
					20 SOPC	12.50	18.39	2.03	84
10 DPPG	5.88	6.39	0.87	47	10 SOPC	12.49	8.78	1.04	41
					10 SOPC	12.52	8.36	0.99	42
					10 SOPC	12.51	8.19	0.97	33
					10 SOPC	12.50	8.28	0.98	29
					10 SOPC	12.51	8.71	1.03	45
					10 SOPC	12.53	8.28	0.98	33

Table S 6: Raw data of precision injections (left: DPPG, right: SOPC). Samples of 100, 200, and 400 µg/mL SOPC and 125, 250, and 500 µg/mL DPPG were injected three times each on three different days.

Injection Name	Retention Time (min) DPPG	Area (pA*min) DPPG	Injection Name	Retention Time (min) SOPC	Area (pA*min) SOPC
DPPG 125.1	5.94	13.15	SOPC 100.1	12.49	9.81
DPPG 125.1	5.96	12.45	SOPC 100.1	12.47	9.82
DPPG 125.1	5.97	11.88	SOPC 100.1	12.48	9.84
DPPG 125.2	6.15	11.93	SOPC 100.2	12.48	10.49
DPPG 125.2	6.16	11.92	SOPC 100.2	12.49	10.49
DPPG 125.2	6.16	11.86	SOPC 100.2	12.49	10.46
DPPG 125.3	6.07	12.20	SOPC 100.3	12.31	10.37
DPPG 125.3	6.07	12.02	SOPC 100.3	12.31	10.41
DPPG 125.3	6.07	12.05	SOPC 100.3	12.32	10.32
DPPG 250.1	6.05	22.31	SOPC 200.1	12.47	19.86
DPPG 250.1	6.06	22.27	SOPC 200.1	12.46	19.78
DPPG 250.1	6.03	22.03	SOPC 200.1	12.47	19.79
DPPG 250.2	6.00	23.83	SOPC 200.2	12.49	20.48
DPPG 250.2	6.00	23.38	SOPC 200.2	12.47	20.32
DPPG 250.2	6.01	23.15	SOPC 200.2	12.48	20.36
DPPG 250.3	5.84	22.23	SOPC 200.3	12.33	20.68
DPPG 250.3	5.87	22.15	SOPC 200.3	12.35	20.77
DPPG 250.3	5.88	22.17	SOPC 200.3	12.35	20.66
DPPG 500.1	5.92	41.50	SOPC 400.1	12.46	36.68
DPPG 500.1	5.93	41.17	SOPC 400.1	12.45	36.75
DPPG 500.1	5.93	41.02	SOPC 400.1	12.46	36.72
DPPG 500.2	5.92	41.67	SOPC 400.2	12.47	37.37
DPPG 500.2	5.93	41.67	SOPC 400.2	12.48	37.30
DPPG 500.2	5.93	41.70	SOPC 400.2	12.47	37.33
DPPG 500.3	5.79	41.61	SOPC 400.3	12.38	36.99
DPPG 500.3	5.80	41.75	SOPC 400.3	12.38	36.89
DPPG 500.3	5.80	41.66	SOPC 400.3	12.40	37.07

Table S 7: Raw data of accuracy injections (left: DPPG, right: SOPC). Samples of 100, 200, and 400 µg/mL DPPG and SOPC of three different stock solutions were injected three times each.

Concentration (µg/mL)	Ret.Time (min) DPPG	Amount (µg/mL) DPPG	Area (pA*min) DPPG	Concentration (µg/mL)	Ret.Time (min) SOPC	Amount (µg/mL) SOPC	Area (pA*min) SOPC
	6.27	104.30	9.84		12.31	100.92	10.37
	6.28	103.56	9.77		12.31	101.31	10.41
	6.30	104.74	9.88		12.32	100.39	10.32
	5.76	100.24	9.48		12.59	97.38	10.02
100	5.76	100.34	9.48	100	12.49	95.51	9.84
	5.76	100.69	9.52		12.50	95.81	9.87
	5.81	98.19	9.29		12.47	101.08	10.39
	5.81	98.43	9.31		12.45	100.87	10.37
	5.82	98.01	9.27		12.45	100.57	10.34
	6.43	205.51	18.72		12.47	200.64	19.86
	6.43	205.27	18.70		12.46	199.78	19.78
	6.42	205.50	18.72		12.47	199.83	19.79
	5.72	200.74	18.31		12.46	198.52	19.67
200	5.73	200.61	18.30	200	12.46	198.05	19.62
	5.74	200.32	18.28		12.47	197.20	19.54
	5.77	202.44	18.46		12.43	208.15	20.55
	5.77	202.53	18.47		12.43	207.27	20.47
	5.78	206.91	18.84		12.41	207.90	20.53
	6.33	404.07	35.00		12.47	405.54	95.65
	6.32	404.04	35.00		12.48	404.77	95.65
	6.32	402.09	34.85		12.47	405.14	95.71
	5.51	402.02	34.84		12.43	401.82	92.18
400	5.52	404.70	35.05	400	12.44	399.42	91.84
	5.53	403.76	34.98		12.43	397.65	92.03
	5.69	391.50	34.01		12.40	426.38	92.47
	5.69	392.18	34.07		12.38	429.74	92.61
	5.69	390.49	33.94		12.41	425.67	92.80

3. Raw data for Fig. 2

Table S8: Total and local DPPG contents in aLUVs prepared at different exchange temperatures. Conversion of ζ to X_{PG}^{out} and determination of lower and upper limits of 95% confidence intervals were carried out using Figure S3.

T_{ex}	5°C					15°C					30°C				
	scrambled aLUVs			aLUVs		scrambled aLUVs			aLUVs		scrambled aLUVs			aLUVs	
	X_{PG}(HPLC) mol%	ζ *mV*	X_{PG}^{out}(ζ) mol%	ζ *mV*	X_{PG}^{out}(ζ) mol%	X_{PG}(HPLC) mol%	ζ *mV*	X_{PG}^{out}(ζ) mol%	ζ *mV*	X_{PG}^{out}(ζ) mol%	X_{PG}(HPLC) mol%	ζ *mV*	X_{PG}^{out}(ζ) mol%	ζ *mV*	X_{PG}^{out}(ζ) mol%
batch 1	10.2			*-33*		10.9			*-32*	27	9.5			*-33*	
batch 2	10.9			*-33*		11.3			*-29*	22	11.6			*-29*	
batch 3	11.4			*-35*		11.0			*-31*	25	9.6			*-27*	
average	**10.8**			***-34***	**32**	**11.1**			***-31***	**26**	**10.2**			***-30***	**24**
s.d.	0.5					0.2					1.0				
lower					28					24					22
upper					45					31					28
batch 4		*-21*	12	*-33*	34		*-21*	12	*-32*	28		*-22*	14	*-32*	28
lower			11		30			11		25			12		25
upper			13		>50			13		34			15		34
batch 5				*-35*	35				*-36*	38				*-34*	33
lower					30					32					28
upper					>50					>50					>50

4. Calibration curve for the zeta potential as a function of the DPPG content of the outer leaflet

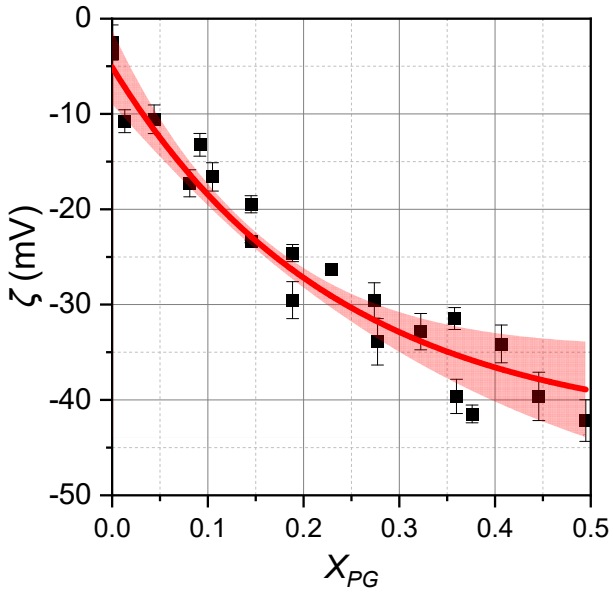

Figure S3: Zeta potential (ζ) calibration curve recorded for symmetrical liposomes of SOPC with different mole fractions of DPPG, X_{PG}, at 25°C. Squares represent a batch of symmetrical liposomes with a certain content of DPPG; errors represent s.d. of three measurements of a given batch. The empirical fit is an instrumentally weighted exponential decay function and the shaded area represents 95%-confidence intervals.

5. The morphology of DVs shown by additional cryo-TEM images

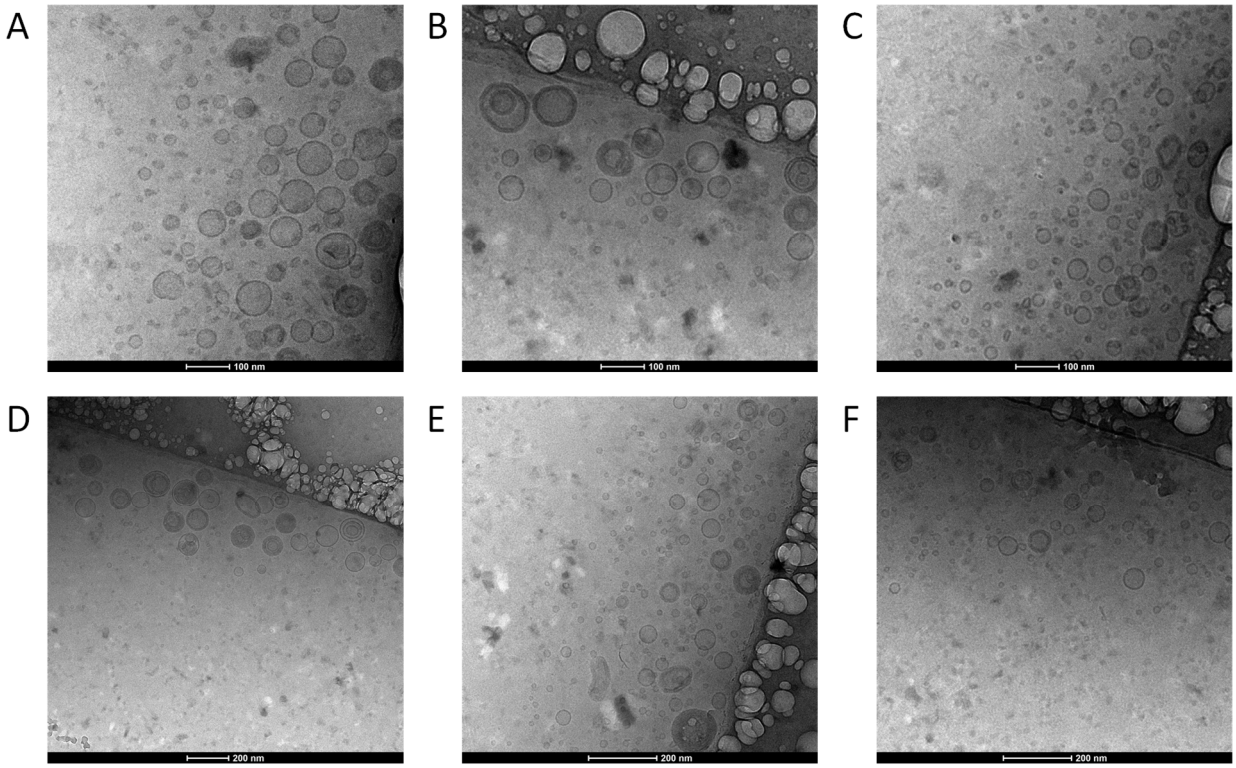

*Figure S4: Multiple cryo-TEM images from aLUVs with 29 mol% DPPGout prepared at T_{ex} = 15°C. Shown is the concurrent existence of spherical MVs and DVs in a 100 nm-scale (**A-C**) and 200 nm-scale (**C-F**). The vesicles were exposed to a temperature increase to 35°C directly after lipid exchange and prior to cryo-TEM imaging.*

6. Details of PPC data of aLUVs prepared at different exchange temperatures

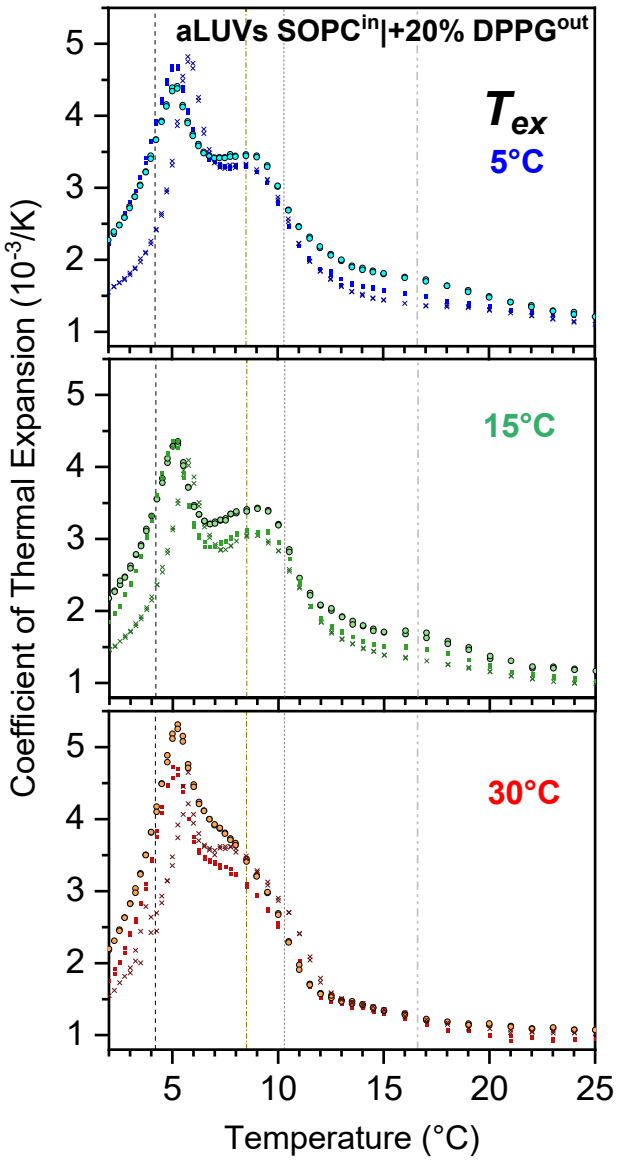

Figure S5: Reproduction of all PPC curves presented in Figure 3B for better resolution of detail. The points represent the individual heat responses of pressure drop and increase after equilibration at a given temperature. Note that crosses, squares and lighter spheres represent three sets of samples prepared at different days, spread over months. Each set of samples was prepared using the same acceptor liposomes and DPPG-cyclodextrin complexes, split in three portions and these thermostatted, mixed and incubated at the different exchange temperatures. The other sets were prepared from scratch, respectively.

7. Review of coupling literature

Table S9: Summary of protein-independent coupling mechanisms reported for free-floating lipid-asymmetric vesicles. Given are the outer leaflet (OUT) and inner leaflet composition (IN), the temperature of lipid exchange (T_{ex}) and experimental observation (T_{obs}), the coupling strength, and observations and methods on which interpretation was based on. Note that the lipid systems listed here are limited to those examined for interleaflet coupling mechanisms in the respective studies. Footnotes are inserted to clarify abbreviations.

OUT [1]	*IN*	T_{ex} / T_{obs}	Coupling strength	Observations	Related methods	Ref.
Dynamic chain interdigitation						
milk-SM (mSM), C24:0-SM	DOPC	55°C / 23°C	Strong coupling	Reduced lateral lipid diffusion *IN*, coupling coefficient mSM/DOPC 0.78 [2]	FCS, FLIM	9
brain-SM (bSM)	POPC, SOPC					
bSM	OMPC					
bSM	DOPC		Weak coupling	Coupling coefficient 0.26 [2]		
mSM	DOPC, Chol	55°C / 25°C–35°C	Strong coupling	L_o domains *IN* and *OUT* in registration, similar lipid packing	CFI	10
eSM			Weak coupling	Differences between lipid packing in L_o and/or L_d domains		
mSM	DPPC	50°C / 50°C	High interdigitation	Increased packing order *IN* and *OUT*	SANS, SAXS	11
MSPC, SMPC, or PMPC	DPPC		Low interdigitation	Increased packing disorder *IN* and/or *OUT*		
POPC, SOPC	DPPC		Matching lateral lipid area of *IN* and *OUT*	Increased packing disorder *IN*		
Membrane undulations						
POPC	POPE and/or POPS	50°C / 50°C	Enhanced coupling	Increased bending rigidity/ bilayer stiffening	NSE, SAXS/SANS	12
POPC, mSM	POPE and/or POPS		Reduced coupling			
mSM or eSM	POPE		No coupling	No anomalous membrane stiffening		
mSM	POPE, POPS					
Intrinsic curvature						
POPE	POPC	35°C or RT / 0–35°C	No coupling	Independent leaflet melting, unaffected acyl chain packing and A_L	DSC, WAXS, SAXS/SANS	13
POPC	POPE					
POPC	POPE		Strong coupling	Cooperative melting, similar packing of *IN* and *OUT*		

Asymmetry stress						
DPPG	SOPC	5°C / 30°C	Weak coupling	Independent leaflet melting	DSC, PPC	this study & unpublished
		15°C / 30°C				
		25°C or 30°C / 30°C	Intermediate coupling	Partially cooperative melting		
	DMPC	25°C / 30°C	Strong coupling	Highly cooperative melting		
Undefined						
SM	DOPC, POPC or POPE/POPS 2:1	55°C / RT	No coupling	Ordered *OUT*, disordered *IN*	FA (DPH, TMA-DPH)	[14]
SM	DOPC, POPC or POPE/POPS 2:1 with Chol		Some degree of coupling	Increased order *IN*		
bSM	bPC or bPC/bPE	65°C /22°C	Physical coupling	Decreased lateral diffusion in both leaflets	FCS	[15]
bSM	DOPC		Lack of coupling	Decreased lateral diffusion *OUT* while unchanged *IN*		
bSM	DOPE/POPS w or w/o Chol	55°C / RT	Weak coupling	Increased order *IN*	FA (DPH, TMA-DPH)	[14]
DPPC	POPC	RT / RT	Some degree of coupling	Reduced lipid packing *OUT* (partly fluidized, larger A_L), disordering of gel-like domains *OUT*	SANS	[16]
DPPC	POPC	RT / 50°C	No transbilayer structural coupling	Unaffected A_L (*asy* and *scr* are in agreement)	SANS/SAXS	[17]
DSPC	DOPC, Chol	55°C or 60°C / 23°C–64°C	No coupling	L_o domain formation *OUT*, weak quenching of DPH fluorescence	FA (DPH, TMA-DPH), FRET	[18]
DPPC, $diC_{15:0}PC$			Intermediate coupling	Intermediate behavior		
DMPC			Strong coupling	No ordered domains *OUT*		
bSM or mSM						

[1] The outer leaflet is enriched with the indicated lipids (thus, not 100% asymmetric); [2] coupling coefficient is calculated as the ratio $(10\ \mu m^2/s - D_{inner})/(10\ \mu m^2/s - D_{outer})$, with D accounting for the relative lateral diffusion coefficient of NBD-DOPE; Acronyms: OUT outer membrane leaflet, IN inner membrane leaflet, T_{ex} exchange temperature, T_{obs} observation temperature, mSM milk-sphingomyelin, bSM brain-SM, eSM egg-SM, bPC brain-phosphatidylcholine, DOPC 1,2-dioleoyl-sn-glycero-3-phosphocholine, OMPC 1-oleoyl-2-myristoyl-sn-glycero-3-PC, DPPC 1,2-dipalmitoyl-sn-glycero-3-PC, MSPC 1-myristoyl-2-stearoyl-sn-glycero-3-PC, SMPC 1-stearoyl-2-myristoyl-sn-glycero-3-PC, PMPC 1-palmitoyl-2-myristoyl-sn-glycero-3-PC, DSPC 1,2-distearoyl-sn-glycero-3-PC, POPC 1-palmitoyl-2-oleoyl-glycero-3-PC, SOPC 1-stearoyl-2-oleoyl-sn-glycero-3-PC, DMPC 1,2-dimyristoyl-sn-glycero-3-PC, DPPG 1,2-dipalmitoyl-sn-glycero-3-phosphoglycerol, DOPE 1,2-dioleoyl-sn-glycero-3-

phosphoethanol-amine, POPE 1-palmitoyl-2-oleoyl-sn-glycero-3-PE, POPS 1-palmitoyl-2-oleoyl-sn-glycero-3-phospho-L-serine, Chol cholesterol, FCS fluorescence correlation spectroscopy, FLIM fluorescence lifetime imaging, CFI confocal fluorescence imaging, FA fluorescence anisotropy, SANS small-angle neutron scattering, SAXS small-angle x-ray scattering, WAXS wide-angle light scattering, DSC differential scanning calorimetry, PPC pressure perturbation calorimetry, NSE neutron spin-echo spectroscopy, FRET Förster resonance energy transfer, asy lipid-asymmetric, scr scrambled (i.e. lipid-symmetric), A_L area per lipid molecule.

References

1 N. Vervoort, D. Daemen and G. Török, *J. Chromatogr. A*, 2008, **1189**, 92–100.

2 *United States Pat. 6,568,245 B2*, 2003.

3 D. Boßmann, B. Bartling, I. de Vries, J. Winkler, H. Neumann, F. Lammers, S. Beutel and T. Scheper, *J. Chromatogr. A*, 2019, **1599**, 85–94.

4 C. Langer and R. Süss, *J. Pharm. Biomed. Anal.*, DOI:10.1016/j.jpba.2021.114120.

5 V. Bender, L. Fuchs and R. Süss, *Int. J. Pharm. X*, 2024, **7**, 100255.

6 European Medicines Agency, Validation of Analytical Procedures Q2(R2), Committee for Medicinal Products for Human Use EMA/CHMP/ICH/82072/2006 (2023), https://database.ich.org/sites/default/files/ICH_Q2%28R2%29_Guideline_2023_1130.pdf.

7 C. Kinsey, T. Lu, A. Deiss, K. Vuolo, L. Klein, R. R. Rustandi and J. W. Loughney, *Electrophoresis*, 2022, **43**, 1091–1100.

8 Y. Mousli, M. Brachet, J. L. Chain and L. Ferey, *J. Pharm. Biomed. Anal.*, 2022, **220**, 115011.

9 S. Chiantia and E. London, *Biophys. J.*, 2012, **103**, 2311–2319.

10 Q. Lin and E. London, *Biophys. J.*, 2015, **108**, 2212–2222.

11 M. P. K. Frewein, P. Piller, E. F. Semeraro, K. C. Batchu, F. A. Heberle, H. L. Scott, Y. Gerelli, L. Porcar and G. Pabst, *J. Membr. Biol.*, 2022, **255**, 407–421.

12 M. P. K. Frewein, P. Piller, E. F. Semeraro, O. Czakkel, Y. Gerelli, L. Porcar and G. Pabst, *Biophys. J.*, 2023, **122**, 2445–2455.

13 B. Eicher, D. Marquardt, F. A. Heberle, I. Letofsky-Papst, G. N. Rechberger, M.-S. Appavou, J. Katsaras and G. Pabst, *Biophys. J.*, 2018, **114**, 146–157.

14 H.-T. Cheng and E. London, *Biophys. J.*, 2011, **100**, 2671–2678.

15 S. Chiantia, P. Schwille, A. S. Klymchenko and E. London, *Biophys. J.*, 2011, **100**, L1–L3.

16 F. A. Heberle, D. Marquardt, M. Doktorova, B. Geier, R. F. Standaert, P. Heftberger, B. Kollmitzer, J. D. Nickels, R. A. Dick, G. W. Feigenson, J. Katsaras, E. London and G. Pabst, *Langmuir*, 2016, **32**, 5195–5200.

17 B. Eicher, F. A. Heberle, D. Marquardt, G. N. Rechberger, J. Katsaras and G. Pabst, *J. Appl. Crystallogr.*, 2017, **50**, 419–429.

18 Q. Wang and E. London, *Biophys. J.*, 2018, **115**, 664–678.